Molecular Interaction of the Antagonist N-(Piperidin-1-yl)-5-(4-chlorophenyl)-1-(2,4-dichlorophenyl)-4-methyl-1H-pyrazole-3-carboxamide with the CB$_1$ Cannabinoid Receptor

Joong-Youn Shim,*[†] William J. Welsh,[‡] Etienne Cartier,[§,||] James L. Edwards,[§,⊥] and Allyn C. Howlett[§,#]

Department of Basic Pharmaceutical Sciences, College of Pharmacy, University of South Carolina, Columbia, South Carolina 29208, Department of Chemistry & Biochemistry and Center for Molecular Electronics, University of Missouri–St. Louis, St. Louis, Missouri 63121, and Department of Pharmacological and Physiological Science, Saint Louis University School of Medicine, St. Louis, Missouri 63104

N-(Piperidin-1-yl)-5-(4-chlorophenyl)-1-(2,4-dichlorophenyl)-4-methyl-1H-pyrazole-3-carbox-amide (SR141716; **1**) is a potent and selective antagonist for the CB$_1$ cannabinoid receptor. Using the AM1 molecular orbital method, conformational analysis of **1** around the pyrazole C3 substituent identified four distinct conformations designated Tg, Ts, Cg, and Cs. The energetic stability of these conformers followed the order Tg > Cg > Ts > Cs for the neutral (unprotonated) form of **1** and Ts > Tg > Cs > Cg for its piperidine N-protonated form. Unified pharmacophore models for the CB$_1$ receptor ligands were developed by incorporating the protonated form of **1** into the superimposition model for the cannabinoid agonists 4-[4-(1,1-dimethylheptyl)-2-hydroxyphenyl]perhydro-2α,6β-dihydroxynaphthalene (CP55244; **2**) and the protonated form of (*R*)-[2,3-dihydro-5-methyl-3-[(4-morpholinyl)methyl]pyrrolo[1,2,3-*de*]-1,4-benzoxazin-6-yl](1-naphthalenyl)methanone (WIN55212-2; **3**) reported previously (Shim et al. In *Rational Drug Design Symposium Series*; Parrill, A. L., Reddy, M. R., Eds.; American Chemical Society: Washington, DC, 1999; pp 165–184). Values of K_i for **1** and a series of 31 structural analogues were determined from radioligand binding analyses by competitive displacement of [^{3}H]CP55940 from cannabinoid receptors in a rat brain membrane preparation. Comparative molecular field analysis (CoMFA) was employed to construct three-dimensional (3D)-quantitative structure–activity relationship (QSAR) models for this data set as unpro-tonated species assuming the Tg, Cg, and Ts conformers and for the protonated species assuming the Ts, Tg, and Cs conformers. Values of the conventional r^2 and cross-validated r^2 (r_{cv}^2) associated with these CoMFA models exceeded the threshold for statistical robustness ($r^2 \geq 0.90$) and internal predictive ability ($r_{cv}^2 \geq 0.50$) in each of these six cases except for the protonated species assuming the Tg conformer (i.e., $r^2 = 0.97$; $r_{cv}^2 = 0.36$). Results from conformational analyses, superimposition models, and 3D-QSAR models suggest that the N1 aromatic ring moiety of **1** dominates the steric binding interaction with the receptor in much the same way as does the C3 alkyl side chain of cannabinoid agonists and the C3 aroyl ring of the aminoalkylindole agonists. We also determined that several of the conformers considered in this study possess the proper spatial orientation and distinct electrostatic character to bind to the CB$_1$ receptor. We propose that the unique region in space occupied by the C5 aromatic ring of **1** might contribute to conferring antagonist activity. We further propose that the pyrazole C3 substituent of **1** might contribute to conferring either neutral antagonist or inverse agonist activity, depending upon the interaction with the receptor.

Introduction

Therapeutically beneficial effects of Δ^9-tetrahydro-cannabinol (Δ^9-THC), a component of *Cannabis sativa*

* To whom correspondence should be addressed. Tel.: 803-576-5684. Fax: 803-777-8356. E-mail: shim@cop.sc.edu.
[†] University of South Carolina.
[‡] University of Missouri–St. Louis. Current address: Department of Pharmacology, Robert Wood Johnson Medical School, University of Medicine & Dentistry of New Jersey, 675 Hoes Lane, Piscataway, NJ 08854.
[§] Saint Louis University School of Medicine.
[||] Current address: Neuroscience Graduate Program, Oregon Health Sciences University, Portland, OR 97201.
[⊥] Current address: Department of Chemistry, University of Florida, Gainesville, FL 32611.
[#] Current address: J. L. Chambers Biomedical/Biotechnology Research Institute, North Carolina Central University, Durham, NC 27707.

extracts, include analgesia, attenuation of nausea and vomiting in cancer chemotherapy, and appetite stimulation in wasting syndromes. Side effects accompanying these therapeutic responses include alterations in cognition and memory, dysphoria/euphoria, and sedation.[1,2] These central nervous system responses to Δ^9-THC are mediated by the guanosine 5′-triphosphate-binding protein (G-protein)-coupled cannabinoid (CB$_1$) receptor in the brain.[3,4] CB$_1$ receptors are activated by multiple chemical classes of cannabimimetic agonists, including: (i) classical ABC-tricyclic analogues, typified by Δ^9-THC; (ii) nonclassical AC-bicyclic and ACD-tricyclic cannabinoid analogues, typified by (−)-3-[2-hydroxy-4-(1,1-dimethyl-heptyl)phenyl]-4-[3-hydroxy-propyl]cyclo-hexan-1-ol (CP55940) and 4-[4-(1,1-dimethylheptyl)-2-
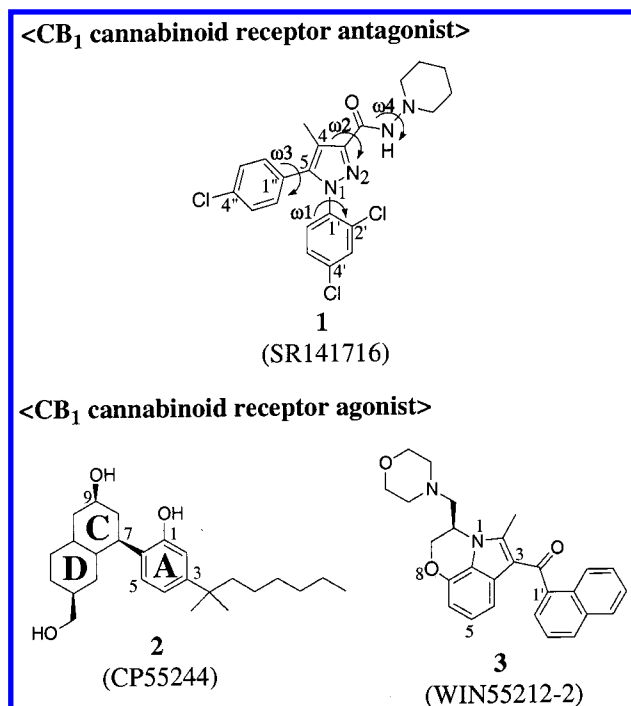
Figure 1. Molecular structures of the CB$_1$ cannabinoid receptor ligands. Compound **1** is a selective CB$_1$ antagonist. Compounds **2** and **3** are nonselective CB$_1$ and CB$_2$ cannabinoid receptor agonists of the nonclassical cannabinoid and AAI chemical classes. The torsion angles for **1** described in the present study are shown as follows: ω1, ω2, ω3, and ω4.

hydroxyphenyl]perhydro-2α,6β-dihydroxynaphthalene (CP55244, **2**; Figure 1), respectively; (iii) aminoalkylindole (AAI) analogues, typified by (*R*)-[2,3-dihydro-5-methyl-3-[(4-morpholinyl)methyl]pyrrolo[1,2,3-*de*]-1,4-benzoxazin-6-yl](1-naphthalenyl)methanone (WIN55212-2, **3**; Figure 1); and (iv) eicosanoid cannabimimetic compounds, typified by arachidonylethanolamide (anandamide). In response to these agonists, the CB$_1$ receptors modulate signaling pathways mediated by adenylate cyclase and protein kinase A, mitogen-activated protein kinases, and ion channels via G-proteins.[5]

Compound **1** (N-(piperidin-1-yl)-5-(4-chlorophenyl)-1-(2,4-dichlorophenyl)-4-methyl-1H-pyrazole-3-carboxamide, SR141716; Figure 1) is a potent and selective arylpyrazole antagonist for the CB$_1$ receptors.[6] Compound **1** exhibits a 500-fold greater affinity in rat brain membranes over spleen membranes in the [^{3}H]CP55940 binding assay.[7] Compound **1** blocks the inhibitory activity of adenylate cyclase caused by cannabinoid agonists,[8] reverses behavioral responses to cannabinoid agonists in rodents,[7,9] blocks the discriminative stimulus effects of cannabinoid agonists in rats and monkeys,[10] and precipitates withdrawal in rats made tolerant to Δ^9-THC.[11,12] In addition to antagonizing the effects of cannabinoid receptor agonists, **1** exhibits "inverse agonist" activity (i.e., compound **1** promotes signal transduction responses that are opposite to those promoted by agonists) in in vitro assay systems.[13-15]

As suggested from the competitive binding of **1** in the [^{3}H]CP55940 assay,[7,15-17] **1** appears to compete with cannabinoid agonists for common binding site(s) on the CB$_1$ receptor. Covalent binding of 3-azido (after ultraviolet irradiation) and 3-isothiocyanato analogues of **1** in rat brain membrane preparations was able to reduce specific binding of [^{3}H]CP55940, suggesting that the

irreversibly bound arylpyrazoles obstructed binding sites potentially occupied by the nonclassical cannabinoid agonist.[18] However, a pattern of distinct binding affinities of **1** and its halogenated analogues in the displacement of [^{3}H]CP55940 vs [^{3}H]SR141716 suggests that arylpyrazoles may interact with a unique region in the CB$_1$ receptor.[17]

We posed the working hypothesis that antagonism by **1** is caused by binding to the same region of the receptor as does the agonist but prohibiting the critical agonist-promoted conformational transition of the receptor. To test this, we carried out extensive conformational analysis calculations on **1** to develop a unified superimposition model for the CB$_1$ receptor agonist and antagonist ligands. Having previously developed a superimposition model for the CB$_1$ cannabinoid receptor agonists **2** and **3**,[19] we were able to identify critical pharmacophoric elements for the receptor interaction common to cannabinoid agonists and the antagonist. The K_i values for a series of arylpyrazoles determined from competitive displacement of [^{3}H]CP55940 were analyzed by the method of comparative molecular field analysis (CoMFA).[20] Three-dimensional (3D)-quantitative structure–activity relationship (QSAR) models for **1** and its structural analogues were developed to correlate structural variation with CB$_1$ receptor binding affinity. On the basis of results from conformational analyses, superimposition models, and 3D-QSAR models, a molecular mechanism for **1**'s antagonist and inverse agonist activity is proposed.

Materials and Methods

Compound **1** was subjected to a conformational search using the SPARTAN (version 5.1.0) molecular modeling program[21] implemented on a Silicon Graphics R5000 Indy workstation. Separate conformational analyses were carried out for the unprotonated and the protonated forms of **1**. Each form of **1** was systematically searched using the AM1 molecular orbital procedure[22] with respect to four torsion angles (Figure 1): ω1 (N2–N1–C1'–C2') with 6-fold rotation, ω2 (N2=C3–C=O) with 4-fold rotation, ω3 (C4=C5–C1''–C2'') with 3-fold rotation, and ω4 (C(=O)–N–N–C) with 2-fold rotation. Conformations of **1** (designated Ts, Tg, Cs, and Cg) obtained from the aforementioned systematic conformational search were compared with conformations obtained from extensive Osawa conformational searches[23] (24-fold rotation of ω1, 12-fold rotation of ω2, 24-fold rotation of ω3, and 12-fold rotation of ω4) using the MMFF94 molecular mechanics force field[24] followed by AM1 geometry optimization.

Superimposition models were constructed from the AM1-derived conformations of the piperidine N-protonated form of **1** and **2** and the morpholine N-protonated form of **3**, respectively, using the DISCO[25] (DIStance COmparison) module accessed through SYBYL (version 6.3).[26] Similar criteria for selecting superimposition models were adopted from our previous work on the cannabinoid agonists.[19] Certain predefined pharmacophoric features were assigned, including hydrophobic atoms or groups, hydrogen bond donor and acceptor atoms, and their respective hydrogen bond acceptor and donor sites. Conformers of **1** and **3** were then identified whose pharmacophoric features were commonly matched to those of the reference conformation of **2** within a specified tolerance limit of 1.0 Å for intramolecular pharmacophoric distances. On the basis of the best-fit superimposition models, putative critical pharmacophoric elements were determined.

Affinities of analogues of **1** for cannabinoid receptors were determined by heterologous displacement of [^{3}H]CP55940 specific binding using rat brain membranes, and K_i values were calculated using assumptions of competitive inhibition

Table 1. Binding Affinity of **1** and Its Analogues[a] for the CB$_1$ Receptor
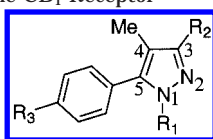
compd	R$_1$	R$_2$	R$_3$	K$_i$ (in nM)[b]	lit. K$_i$ (in nM)[c]
1 (SR141716)	2,4-dichlorophenyl	N-(piperidin-1-yl)amido	Cl	1.3	11.5
4	2,4-dichlorophenyl	N-(piperidin-1-yl)amido	I	6	7.49
5	4-chlorophenyl	N-(piperidin-1-yl)amido	Cl	55	60.4
6	4-nitrophenyl	N-(piperidin-1-yl)amido	Cl	109	
7	4-aminophenyl	N-(piperidin-1-yl)amido	Cl	72	
8	2,4-dichlorophenyl	N-(cyclohexyl)amido	Br	15	11.7
9	2,4-dichlorophenyl	N-(cyclohexyl)-N-methylamido	Br	56	76.7
10	2,4-dichlorophenyl	N-(hydroxyethyl)amido	Br	165	1120
11	2,4-dichlorophenyl	N-(morpholin-4-yl)amido	Br	19	53.9
12	cyclohexyl	N-(piperidin-1-yl)amido	H	391	
13	*n*-propyl	N-(piperidin-1-yl)amido	H	771	
14	*n*-butyl	N-(piperidin-1-yl)amido	H	187	
15	*n*-pentyl	N-(piperidin-1-yl)amido	H	23	
16	*n*-pentyl	N-(piperidin-1-yl)amido	Br	63	
17	*n*-hexyl	N-(piperidin-1-yl)amido	H	21	
18	*n*-heptyl	N-(piperidin-1-yl)amido	H	47	
19	2,4-dichlorophenyl	(piperidin-1-yl)ethoxymethyl	Cl	232	
20	2,4-dichlorophenyl	(cyclohexyl)methoxymethyl	Cl	100	
21	2,4-dichlorophenyl	4-fluorobenzoxymethyl	Cl	6	
22	2,4-dichlorophenyl	N-*n*-pentyl-amido	Cl	3	
23	2,4-dichlorophenyl	N-*n*-heptyl-amido	Cl	3	
24	2,4-dichlorophenyl	pentylcarbonyl	Cl	25	
25	4-*sec*-butylphenyl	N-(piperidin-1-yl)amido	Cl	37	
26	4-*n*-butylphenyl	N-(piperidin-1-yl)amido	Cl	256	
27	4-*n*-pentylphenyl	N-(piperidin-1-yl)amido	Cl	1360	
28	2,4-dichlorophenyl	N-(piperidin-1-yl)amido	*n*-pentyl	1	
31[d,e]	2-chlorophenyl	phenylamido	acetyl	7	
32[e]	2,4-dichlorophenyl	N-(piperidin-1-yl)amido	ethyl[f]		183
33[e]	2,4-dichlorophenyl	phenylamido	Br		31.1
34[e]	2,4-dichlorophenyl	N-(piperidin-1-yl)amido	H		123
35[e]	2,4-dichlorophenyl	N-(pyrrolidin-1-yl)amido	Br		17.1
36[e]	2,4-dichlorophenyl	N-(piperidin-1-yl)amido	Br		16.8
37[e]	2,4-dichlorophenyl	N-(homopiperidin-1-yl)amido	Br		7.85
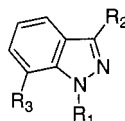
compd	R$_1$	R$_2$	R$_3$	K$_i$ (nM)[g]
29	2,4-dichlorophenyl	N-(piperidin-1-yl)amido	Cl	746
30	2,4-dichlorophenyl	N-(piperidin-1-yl)amido	NO$_2$	202

[a] These compounds, except where indicated, were used as the training set to construct CoMFA models 1−6, whereas compounds **31**−**37** were used as the test set compounds. The K$_i$ values for inhibition of [^{3}H]CP55940 binding to the CB$_1$ receptor in rat brain membranes were determined as described in the text or were taken from ref 16. [b] Present study. [c] Ref 16. [d] −CN instead of −Me at the C4 position. [e] Test set compound. [f] Directly attached to C5. [g] Present study.

as previously described.[15] Data points from three to six individual experiments were combined for nonlinear regression analysis of sigmoid curves (log scale) using Inplot (Graphpad, Inc.). As a measure of variability of the data, the average ratio of the standard error to the EC$_{50}$ values in log units was 0.017 (i.e., average coefficient of variation = 1.7% in log units) for the curves reported in Table 1. Data for the EC$_{50}$ values were converted to K$_i$ values using the assumptions of competitive inhibition (K$_i$ = EC$_{50}$/(1 + CP/K$_{CP}$), where the CP/K$_{CP}$ ratio (concentration of [^{3}H]CP55940/dissociation constant for [^{3}H]-CP55940) varied between 0.7 and 1.0 for this set of experiments.

On the basis of three distinct conformations of the unprotonated form of **1** (Tg, Cg, and Ts), three separate CoMFA models were derived from K$_i$ values on **1** and 27 analogues (Table 1): CoMFA model 1 assuming the Tg form, CoMFA model 2 assuming the Cg form, and CoMFA model 3 assuming the Ts form. Similarly, on the basis of three distinct conformations of the protonated form of **1** (Ts, Tg, and Cs), three separate CoMFA models were derived as follows: CoMFA model 4 assuming the Ts form, CoMFA model 5 assuming the Tg form, and CoMFA model 6 assuming the Cs form. For those

compounds with an additional flexible side chain (i.e., compounds **10** and **13**−**28**), further conformational searches were carried out using MMFF94 for the Tg and Ts forms and AM1 for the Cg and Cs forms to select four or five low-energy conformations to be used for developing CoMFA models. The AM1 method was used for the Cg and Cs forms, since the MMFF failed to find any low-energy conformer associated with the Cg and Cs forms (vide infra). The partial atomic charges required for calculating the electrostatic interactions were assigned using the Gasteiger−Marsili formalism[27] for the Ts and Tg forms and the AM1-derived electrostatic-potential fitted charges for the Cg and Cs forms. Compound **1** was selected as the template molecule for aligning each compound in the training set by root mean square (RMS) fitting onto the pyrazole ring five atoms. Implementing standard CoMFA procedures, a probe represented by a carbon atom with radius 1.53 Å and +1 charge was used to explore the steric (van der Waals) and electrostatic (Coulombic) fields around the training set of molecules aligned within a 3D lattice. A distance-dependent dielectric expression ($\epsilon = \epsilon_0 r$, with $\epsilon_0 = 1$) was used for calculating the electrostatic field values. Partial least squares (PLS) regression[28] was employed to correlate these
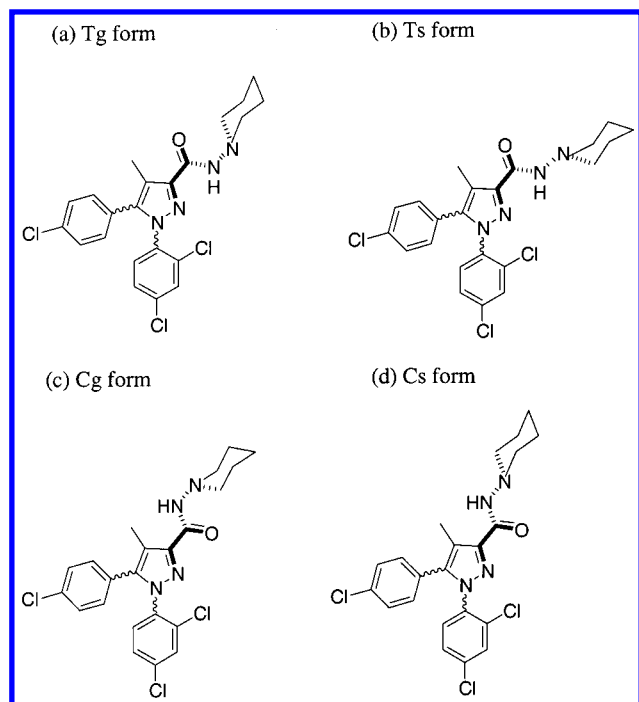
Figure 2. Four distinctive low-energy conformers of **1** defined by the torsion angles $\omega 2$ (N2=C3−C=O) and $\omega 4$ (C(=O)−N−N−C), as determined by AM1 calculations using conformational search approaches. Bonds involved in $\omega 2$ are represented with bold solid lines, and bonds involved in $\omega 4$ are represented with dotted lines. The $\omega 4$ angle is about 120° for the s form and about −60° for the g form.

field values with the negative logarithm of the observed K_i values (pK_i) in units of nanomolar. The "leave-one-out" cross-validation procedure[29] with column filtering of 2.0 kcal/mol was employed to derive the CoMFA models. The PLS analysis was repeated using each conformation among the multiple low-energy conformations of the training set compounds to yield the highest cross-validated r^2 (r_{cv}^2) and to determine the optimum number of principal components. The PLS analysis was then repeated without cross-validation to obtain a predictive model and associated conventional r^2 values, from which the CoMFA coefficient contour plots for the steric and electrostatic potentials were generated.

Compounds **1** and **31** were obtained from Dr. John Lowe at Pfizer, Inc.[10,12,15] Samples of the arylpyrazole analogues were provided courtesy of Drs. A. Makriyannis[16] and R. Razdan.[30]

Results

Conformational Analysis. Conformational analysis of **1** was carried out using the AM1 method. With respect to torsion angles $\omega 2$ and $\omega 4$ (Figure 1), conformations of **1** were classified into four different forms: Tg, Ts, Cg, and Cs forms (Figure 2). The first letter T or C refers to s-trans or s-cis associated with torsion angle $\omega 2$, whereas the second letter s or g refers to skew or gauche associated with torsion angle $\omega 4$ (ca. +120° for the s form and ca. −60° for the g form). For the unprotonated form, the energetically most stable conformation was the Tg form, which was approximately 2, 5, and 7 kcal/mol more stable than the Cg, Ts, and Cs forms, respectively (Table 2a). Consistent with the AM1 results, ab initio calculations at the HF/3-21G* level of theory revealed that the Tg form was energetically the most stable and approximately 10 kcal/mol more stable than the Cg form. Contrary to the AM1 results, the HF/3-21G* results showed that the Ts form was 8 kcal/mol more stable than the Cg form. Additional

conformers from the AM1 method having the piperidinyl ring plane planar to the amide plane were considered to be unstable conformations based on the HF/3-21G* results. In the case of the protonated form, the energetically most stable conformation was the Ts form, which was approximately 3, 4, and 7 kcal/mol more stable than the Tg, Cs, and Cg forms, respectively (Table 2b). Consistent with the AM1 results, ab initio calculations at the HF/3-21G* level of theory revealed that the Ts form was energetically the most stable and approximately 9 kcal/mol more stable than the Cs form. Only the Ts and Tg conformations were found from extensive Osawa and systematic conformational searches using the MMFF94 force field followed by AM1 full optimization. The MMFF94 calculations found no energy minimum near $\omega 2 = 0°$ (s-cis) that would correspond to the Cs and Cg forms.

Possible conformations of **1** in either its unprotonated or its protonated form were explored. In an isolated environment, the piperidine ring would exhibit a pK_a of 11 at 25 °C and would be predominantly protonated at physiological pH. However, closer inspection of **1** reveals that the molecule is extensively conjugated and, more specifically, that its piperidine ring is bonded directly to an electron-withdrawing amide group and an electron-donating imidazole ring. These two factors would act to modulate the basicity of the piperidine N atom significantly, making it difficult for us to predict unequivocally whether the unprotonated or protonated form of **1** would dominate under physiological conditions. In consideration of the fact that the biologically active form of **1** and its structural analogues may be unprotonated, protonated, or either way, we constructed separate 3D-QSAR models for both the unprotonated and the protonated forms of this data set of compounds.

In the unprotonated form, the energetically preferred conformation places the piperidine nitrogen lone pair of electrons on the opposite side (i.e., g form) rather than on the same side (i.e., s form) of the amide oxygen. As shown in Figure 3a, the s form would experience an unfavorable dipole−dipole interaction between the amide oxygen and the piperidine nitrogen. Consistently, AM1 calculations on **1** in its unprotonated form indicate that the g form is approximately 5 kcal/mol more stable than the s form. In contrast, the protonated form prefers conformations such that the proton on the piperidine nitrogen is positioned on the same side (i.e., s form) rather than the opposite side of the amide oxygen (i.e., g form) (Figure 3b). The s form is likely stabilized by electrostatic and/or hydrogen-bonding interactions between the amide O atom and the piperidine N−H. Consistently, AM1 calculations predict that the s form is preferred over the g form by 3 kcal/mol.

Superimposition of 1 onto Cannabinoid Agonists. It was postulated that superimposition of the potent agonists **2** and **3** and the potent antagonist **1** might reveal common elements that are key for CB$_1$ receptor−ligand binding. More importantly, a superimposition could be valuable in predicting moieties unique to **1** that inhibit the receptor from engaging in conformational changes essential for activation and moieties unique to agonists that are necessary for activation. We began with the superimposition model for **2** and **3** developed by the authors in an earlier study.[19] Employ-

Table 2. Low-Energy Conformations of **1** Found by Systematic Conformational Search of the Torsion Angles (in Degrees) $\omega 1$, $\omega 2$, $\omega 3$, and $\omega 4$, Using the AM1 Method

(a) assumed as an unprotonated species					
conformer	E_{rel} (kcal/mol)	$\omega 1$ (N2−N1−C1′−C2′)	$\omega 2$ (N2=C3−C=O)	$\omega 3^a$ (C4=C5−C1″−C2″)	$\omega 4$ (C(=O)−N−N−C)
Tg Forms					
CNF_1[b]	0.00	60.3	147.8	57.6	71.3
CNF_2	0.01	−62.8	−151.0	119.8	54.2
CNF_3	0.05	67.5	−153.7	44.4	54.4
CNF_4	0.22	−63.5	157.6	118.2	71.5
CNF_5	0.27	−99.5	−148.8	42.5	54.6
CNF_6	0.28	98.7	145.2	134.9	71.4
CNF_7	0.32	−96.3	165.1	43.4	72.3
CNF_8[c]	0.33	95.1	−159.8	136.3	54.4
CNF_9	0.35	55.1	−149.5	78.7	54.8
Cg Forms					
CNF_10	2.29	64.5	48.8	56.6	73.3
CNF_11	2.32	−99.1	−44.1	44.7	53.6
CNF_12	2.41	−64.2	45.7	131.5	73.2
CNF_13	2.47	−63.3	−48.1	119.1	73.7
CNF_14	2.72	−95.7	43.2	54.5	73.3
CNF_15	2.74	97.6	−41.4	126.7	54.0
Ts Forms					
CNF_16	4.67	60.2	143.1	57.7	134.2
CNF_17	4.76	−64.8	145.0	134.1	134.9
CNF_18[d]	4.78	63.6	−143.8	44.5	105.6
CNF_19	4.93	−98.7	−142.2	42.8	103.6
CNF_20	4.98	101.6	139.9	136.5	124.3
CNF_21[e]	5.14	90.1	−147.7	123.2	99.4
CNF_22	5.15	−95.1	150.3	52.9	136.6
Cs Forms					
CNF_23	7.28	−64.2	−51.6	119.8	127.2
CNF_24	7.33	−103.2	−50.7	42.7	126.8
CNF_25	7.42	62.5	−51.1	43.8	127.3
CNF_26	7.59	−93.3	57.5	52.9	136.7
CNF_27	7.64	95.0	−50.8	122.9	127.0
(b) assumed as a protonated species					
conformer	E_{rel} (kcal/mol)	$\omega 1$ (N2−N1−C1′−C2′)	$\omega 2$ (N2=C3−C=O)	$\omega 3^f$ (C4=C5−C1″−C2″)	$\omega 4$ (C(=O)−N−N−C)
Ts Forms					
CNF_1	0.00	−65.0	−173.6	119.3	117.7
CNF_2	0.00	64.5	174.7	59.6	117.8
CNF_3[g]	0.02	−67.7	−176.7	131.2	117.9
CNF_4[h]	0.02	68.1	176.4	46.5	117.2
CNF_5[i]	0.40	−92.9	−175.4	45.8	117.5
CNF_6[j]	0.40	92.5	174.7	132.2	117.3
CNF_7	0.41	87.6	179.2	120.9	117.7
CNF_8	0.41	−86.6	179.9	58.4	117.1
Tg Forms					
CNF_9	2.50	64.2	174.2	59.5	−62.4
CNF_10	2.50	−63.4	−173.1	118.6	−62.4
CNF_11	2.52	−67.8	−176.3	131.1	−62.4
CNF_12	2.52	68.5	176.8	46.9	−62.4
CNF_13	2.90	92.5	174.3	132.0	−62.5
CNF_14	2.90	−93.1	−175.0	46.1	−62.5
CNF_15	2.92	−85.8	−178.1	58.9	−62.5
CNF_16	2.92	85.8	177.2	119.6	−62.5
Cs Forms					
CNF_17	4.19	−78.4	−36.4	118.8	117.3
CNF_18	4.19	77.9	36.3	59.8	117.6
CNF_19	4.46	97.8	35.0	131.2	117.3
CNF_20	4.46	−97.8	−35.0	47.2	117.6
CNF_21	4.54	−70.3	31.8	128.4	116.7
CNF_22	4.54	71.5	−32.4	49.7	117.9
Cg Forms					
CNF_23	6.43	77.9	37.6	59.9	−62.4
CNF_24	6.69	−97.4	−36.8	47.0	−62.3
CNF_25	6.69	97.5	36.9	131.4	−62.3
CNF_26	6.77	−70.2	34.4	128.7	−62.3
CNF_27	6.77	68.6	−34.6	49.8	−62.4
CNF_28	6.91	−62.3	34.5	−78.5	−62.3
CNF_29	6.94	−88.6	35.1	60.0	−62.3
CNF_30	6.94	87.8	−34.3	−60.2	−62.1

[a] The conformation with a positive $\omega 3$ is listed here, whereas an equivalent conformation arising from the 2-fold symmetry of the 4-chlorophenyl moiety is omitted. [b] AM1 optimized conformation of the 1st lowest energy conformer from the systematic conformational search using MMFF. [c] AM1 optimized conformation of the 3rd lowest energy conformer from the systematic conformational search using MMFF. [d] AM1 optimized conformation of the 2nd lowest energy conformer from the systematic conformational search using MMFF. [e] AM1 optimized conformation of the 4th lowest energy conformer from the systematic conformational search using MMFF. [f] The conformation with a positive $\omega 3$ is listed here, whereas an equivalent conformation arising from the 2-fold symmetry of the 4-chlorophenyl moiety is omitted. [g] AM1 optimized conformation of the 2nd lowest energy conformer from the Osawa conformational search. AM1 optimized conformation of the 6th lowest conformer from the Osawa search was similar to this conformation with $\omega 4 = 114.2°$. [h] AM1 optimized conformation of the 1st lowest energy conformer from the Osawa conformational search. AM1 optimized conformation of 5th lowest conformer from the Osawa search was similar to this conformation with $\omega 4 = 120.0°$. [i] AM1 optimized conformation of the 3rd lowest energy conformer from the Osawa conformational search. AM1 optimized conformation of 7th lowest conformer from the Osawa search was similar to this conformation with $\omega 4 = 114.0°$. [j] AM1 optimized conformation of the 4th lowest energy conformer from the Osawa conformational search. AM1 optimized conformation of 8th lowest conformer from the Osawa search was similar to this conformation with $\omega 4 = 120.2°$.
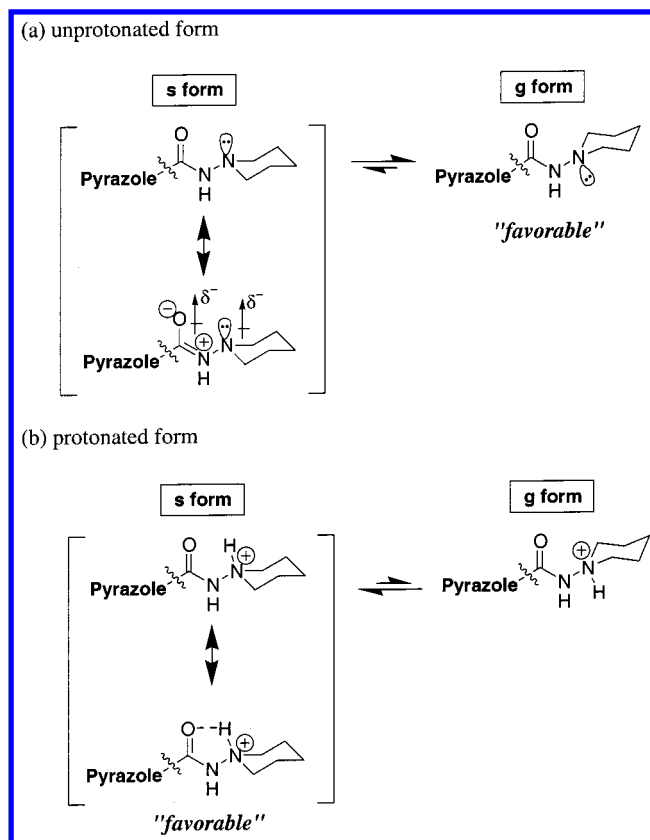
Figure 3. Conformers of **1** with respect to torsion angle $\omega 4$ (C(=O)−N−N−C), assumed as (a) unprotonated species and (b) protonated species.

ing DISCO and Sybyl "field fit" procedures, this model was based on several criteria: (i) overlap of the C3 dimethylheptyl side chain of **2** with the C3 aroyl ring moiety of **3**, (ii) the number of pharmacophoric elements, (iii) the RMS fit of corresponding pharmacophoric elements, and (iv) the degree of overlap of molecular volumes.[19] In that study, it was found that both the Z (i.e., s-trans) and the C (i.e., s-cis) conformations for **3** with respect to torsion angle $\tau 1$ (C2=C3−C=O) were capable of satisfying those interactions with the receptor deemed essential for high affinity binding. Both Z and
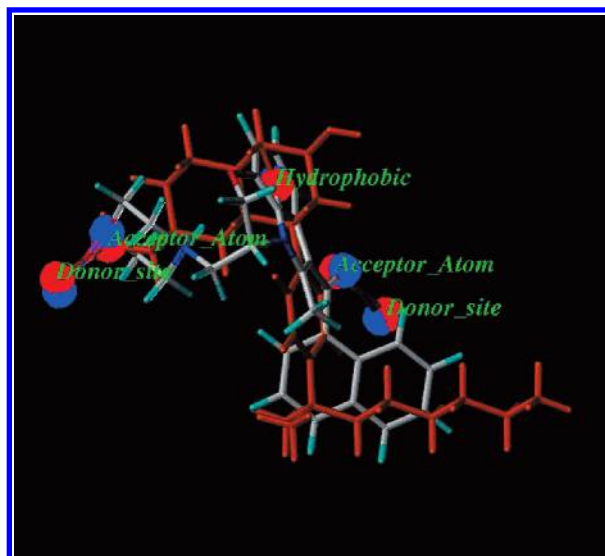

Figure 4. DISCO-derived Z superimposition model for compounds **2** and **3**.

C models predicted a high degree of overlap between the C3 side chain of **2** and the C3 aroyl ring moiety of **3**, consistent with the prediction that steric interactions contribute significantly to the binding affinities for both cannabinoid[31] and AAI[32] agonists. Additionally, the pharmacophore for both Z and C models identified the A-ring hydroxyl oxygen of **2** as a hydrogen bond acceptor corresponding to the C3 aroyl oxygen of **3**.[19] Selection of the Z model was justified based on three observations: (i) it shares greater molecular volume overlap with **2** (156 Å³), (ii) it shares a greater number of pharmacophoric features in common with **2**, and (iii) the Z conformation is consistent with the known SAR for the N1 side chain of the AAIs and the B- and D-rings of the classical and nonclassical cannabinoids.[19] The remaining key pharmacophoric features incorporated in the Z model included a hydrophobic center for the C-ring of **2** corresponding to the benzene ring of the indole in **3** and an oxygen acceptor atom in the D-ring hydroxyl of **2** corresponding to the morpholino oxygen atom of **3** (Figure 4).

Table 3. Two Distinctive Superimposition Models (model A and model B) of Compounds **1**−**3** Identified by DISCO

conformer of the protonated form of **1**	model A		model B
	CNF_5 (Ts form)	CNF_9 (Tg form)	CNF_18 (Cs form)
$\omega 2$ (N2=C3−C=O) (deg)	−175.4	174.2	36.3
$\omega 4$ (C(=O)−N−N−C) (deg)	117.5	−62.4	117.6
relative energy (kcal/mol)	0.40	2.50	4.19

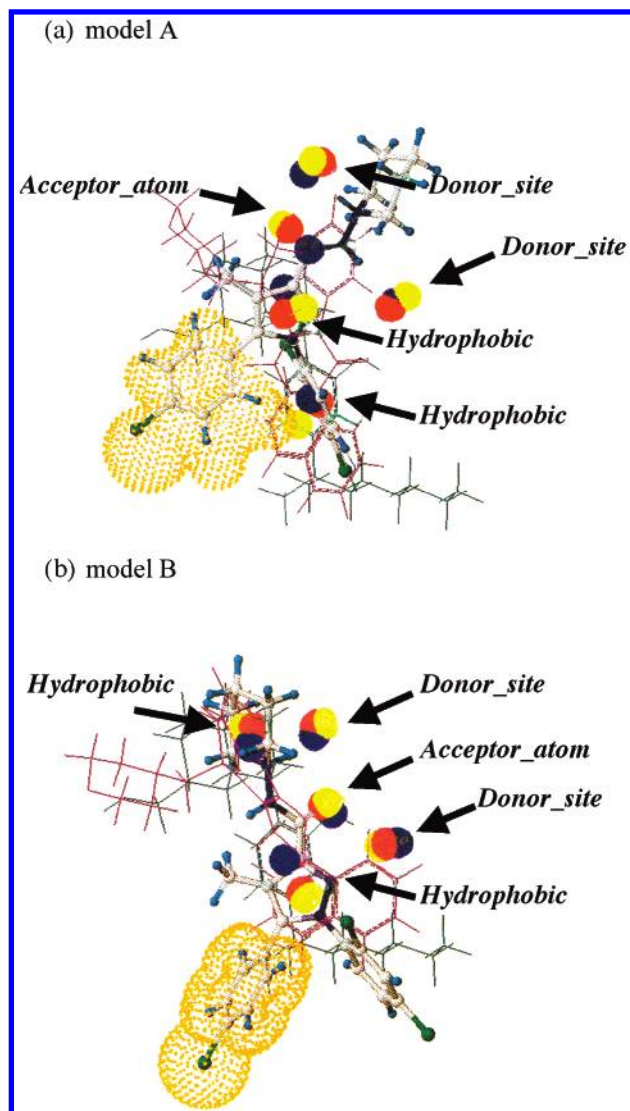| DISCO results	model A		model B
	CNF_5 (Ts form)	CNF_9 (Tg form)	CNF_18 (Cs form)
pharmacophoric features in terms of compd **1**	N1 aryl ring centroid (i) 1 hydrophobic center pyrazole ring centroid (ii) 1 hydrophobic center amide oxygen (iii) 1 acceptor atom (iv) 1 donor site N2 (v) 1 donor site		pyrazole ring centroid (i) 1 hydrophobic center piperidine ring centroid (ii) 1 hydrophobic center amide oxygen (iii) 1 acceptor atom (iv), (v) 2 donor sites
RMSD (compd **2**) (Å)	0.88	0.89	0.77
RMSD (compd **3**) (Å)	0.72	0.70	0.28
overlap volume (compd **2**) (Å³)	111	102	180
overlap volume (compd **3**) (Å³)	128	126	129

Figure 5. DISCO-derived superimposition of compounds **2**, **3**, and **1** using conformer CNF_5 for model A (a) and conformer CNF_18 for model B (b) of the protonated form of **1**. Compound **1** is colored by atom type, whereas **2** is colored in green and **3** is colored in purple. The pharmacophoric features of the reference molecules of **1**−**3** are represented as red, blue, and yellow spheres, respectively. A van der Waals volume of the C5 aryl ring moiety of **1** is represented with orange dots.

Superimposition models incorporating the protonated form of **1** (Table 2b), **2**, and the protonated form of **3** were constructed from the AM1-derived conformations using the DISCO program. Two distinct superimposition models, designated model A and model B, were derived (Figure 5a,b, respectively). Model A was derived from CNF_5 (a Ts form), and model B was derived from CNF_18 (a Cs form) of **1**. Properties of these two superimposition models are summarized in Table 3. A superimposition model derived from CNF_9 (a Tg form) was quite similar to model A, for the 3D pharmacophoric features of the Ts and Tg forms differ only with respect to the piperidinyl ring on the C3 amide group (i.e., associated with torsion angle $\omega 4$).

As shown in Figure 5a, model A identified the following common pharmacophoric elements in **1**−**3**: (a) a hydrophobic center (the N1 aryl ring of **1**, the A-ring

of **2**, and the C3 aroyl ring of **3**); (b) a second hydrophobic center (the pyrazole ring of **1**, the C-ring of **2**, and the indole ring of **3**); (c) a hydrogen bond acceptor atom (the amide oxygen of **1**, the C-ring hydroxyl oxygen of **2**, and O8 of **3**); (d) a hydrogen bond donor site within the putative receptor binding pocket that would partner with c; and (e) a second hydrogen bond donor site within the receptor binding pocket that would partner with the N2 of **1**, the A-ring hydroxyl oxygen of **2**, and the C3 aroyl oxygen of **3**, respectively. Compound **1** overlaps better with **3** than with **2** in model A, largely because the N1 aryl ring of **1** fails to extend more than two carbon atom lengths beyond the A-ring of **2** and because the constituent extending beyond the amide oxygen of **1** has no comparable constituent in the nonclassical cannabinoids in this model.

Model B identified the following pharmacophoric elements: (a) a hydrophobic center (the pyrazole ring of **1**, the A-ring of **2**, and the C3 aroyl ring of **3**); (b) a second hydrophobic center (the piperidine ring of **1**, the C-ring of **2**, and the benzene ring moiety of the **3** indole); (c) a hydrogen bond acceptor atom (the amide oxygen of **1**, the A-ring hydroxyl oxygen of **2**, and C3 aroyl oxygen of **3**); and (d) a hydrogen bond donor site within the receptor binding pocket that would partner with c. Molecular overlap appears better with **2** than with **3** in model B. Both models show alignment of the N1 aryl ring moiety of **1** with the C3 side chain of **2** and the C3 aroyl ring moiety of **3**. However, in model B, the N1 aryl ring is not identified as one of the hydrophobic centers but is displaced downward along the C3 dimethylheptyl side chain of the cannabinoid structure. Consensus from a number of studies indicates that the C3 alkyl side chain of cannabinoid structures attains a configuration that is perpendicular to the A-ring.[33,34] Thus, the importance of the **1** constituent at the N1 aryl position has been considered using additional methodology (see below).

3D-QSAR Models for 1 and its Analogues. The CoMFA method was employed to build 3D-QSAR models for **1** and its analogues based on observed binding affinities (K_i values) for displacement of the cannabinoid [³H]CP55940. A total of six separate CoMFA models were constructed, corresponding to the Tg (model 1), Cg (model 2), and Ts (model 3) conformers assuming the unprotonated species and to the Ts (model 4), Tg (model 5), and Cs (model 6) conformers assuming the protonated species. In each case, the best model was derived by exhaustively checking each conformation of the training set compounds (a total of 110 conformations from 28 training set compounds). Observed vs CoMFA-predicted pK_i values for these training set compounds are represented in Table 4.

Corresponding values of the conventional r^2 and r_{cv}^2 associated with these CoMFA models for the training set of compounds as unprotonated species were 0.97 and 0.68 for model 1 (Tg), 0.95 and 0.73 for model 2 (Cg), and 0.96 and 0.69 for model 3 (Ts). The r_{cv}^2 values are all well above the standard criterion ($r_{cv}^2 \geq 0.50$) required for predictive ability and too similar to distinguish among models 1−3 on the basis of statistical quality. Hence, comparison of the statistical parameters associated with these models (Table 5) does not reflect particular preference for one conformer over another.

Table 4. Observed vs CoMFA-Predicted pK_i Values in Units of Nanomolar for the Training Set of 28 Compounds

(a) assumed as unprotonated species

compd	pK_i obsd	CoMFA model 1 (Tg form)		CoMFA model 2 (Cg form)		CoMFA model 3 (Ts form)	
		pred	residual	pred	residual	pred	residual
1 (SR141716)	0.00	−0.53	0.53	−0.62	0.62	−0.61	0.61
4	−0.78	−0.45	−0.33	−0.65	−0.13	−0.60	−0.18
5	−1.74	−1.81	0.07	−1.83	0.09	−1.79	0.05
6	−2.04	−1.85	−0.18	−1.98	−0.06	−1.95	−0.09
7	−1.86	−1.86	0.00	−1.74	−0.12	−1.73	−0.13
8	−1.18	−1.09	−0.08	−1.07	−0.11	−1.10	−0.08
9	−1.75	−1.82	0.08	−1.77	0.02	−1.76	0.01
10	−2.22	−2.35	0.13	−1.66	−0.56	−2.34	0.12
11	−1.28	−1.34	0.06	−1.09	−0.19	−1.25	−0.03
12	−2.59	−2.57	−0.02	−2.72	0.13	−2.80	0.20
13	−2.89	−2.96	0.07	−2.85	−0.04	−2.80	−0.09
14	−2.27	−2.22	−0.05	−2.39	0.12	−2.26	−0.01
15	−1.36	−1.34	−0.02	−1.59	0.23	−1.34	−0.02
16	−1.80	−1.88	0.08	−1.86	0.06	−1.82	0.02
17	−1.32	−1.29	−0.03	−1.26	−0.06	−1.13	−0.19
18	−1.67	−1.64	−0.03	−1.66	−0.01	−1.76	0.09
19	−2.37	−2.38	0.01	−2.37	0.00	−2.45	−0.08
20	−2.00	−1.97	−0.03	−2.12	0.12	−1.94	−0.06
21	−0.78	−0.73	−0.05	−0.85	0.07	−0.78	0.00
22	−0.48	−0.47	−0.01	−0.56	0.08	−0.46	−0.02
23	−0.48	−0.37	−0.11	−0.43	−0.05	−0.39	−0.09
24	−1.40	−1.36	−0.04	−1.43	0.03	−1.22	−0.17
25	−1.57	−1.52	−0.05	−1.35	−0.22	−1.50	−0.07
26	−2.41	−2.49	0.08	−2.58	0.17	−2.60	0.19
27	−3.13	−3.11	−0.02	−3.03	−0.10	−3.01	−0.13
28	0.00	−0.06	0.06	0.06	−0.06	−0.04	0.04
29	−2.87	−2.75	−0.12	−2.92	0.05	−2.75	−0.12
30	−2.31	−2.31	0.00	−2.21	−0.10	−2.34	0.03

(b) assumed as protonated species

compd	pK_i obsd	CoMFA model 4 (Ts form)		CoMFA model 5 (Tg form)		CoMFA model 6 (Cs form)	
		pred	residual	pred	residual	pred	residual
1 (SR141716)	0.00	−0.48	0.48	0.04	−0.04	−0.60	0.60
4	−0.78	−0.46	−0.32	−0.98	0.20	−0.62	−0.15
5	−1.74	−1.95	0.21	−1.77	0.03	−1.81	0.07
6	−2.04	−1.99	−0.05	−1.84	−0.20	−2.03	−0.01
7	−1.86	−1.71	−0.15	−1.79	−0.07	−1.79	−0.06
8	−1.18	−1.09	−0.08	−1.21	0.03	−1.17	−0.01
9	−1.75	−1.70	−0.05	−1.71	−0.03	−1.91	0.16
10	−2.22	−2.32	0.10	−2.27	0.05	−2.37	0.15
11	−1.28	−1.08	−0.20	−1.22	−0.06	−1.00	−0.28
12	−2.59	−2.67	0.08	−2.75	0.16	−2.69	0.10
13	−2.89	−2.73	−0.16	−2.77	−0.12	−2.91	0.02
14	−2.27	−2.53	0.25	−2.33	0.05	−2.23	−0.04
15	−1.36	−1.56	0.19	−1.76	0.40	−1.45	0.09
16	−1.80	−1.91	0.11	−1.54	−0.26	−1.81	0.01
17	−1.32	−1.22	−0.10	−1.21	−0.11	−1.22	−0.10
18	−1.67	−1.58	−0.09	−1.62	−0.05	−1.55	−0.12
19	−2.37	−2.35	−0.01	−2.30	−0.06	−2.33	−0.03
20	−2.00	−1.96	−0.04	−2.04	0.04	−2.03	0.03
21	−0.78	−0.67	−0.11	−0.78	0.00	−0.62	−0.15
22	−0.48	−0.52	0.04	−0.46	−0.02	−0.45	−0.03
23	−0.48	−0.53	0.06	−0.39	−0.08	−0.35	−0.13
24	−1.40	−1.47	0.07	−1.39	−0.01	−1.41	0.01
25	−1.57	−1.47	−0.09	−1.61	0.04	−1.48	−0.08
26	−2.41	−2.62	0.21	−2.65	0.24	−2.52	0.12
27	−3.13	−3.03	−0.11	−3.02	−0.11	−3.05	−0.09
28	0.00	−0.03	0.03	−0.11	0.11	0.00	0.00
29	−2.87	−2.60	−0.27	−2.55	−0.32	−2.65	−0.22
30	−2.31	−2.31	0.00	−2.48	0.17	−2.33	0.02

Corresponding values of the conventional r^2 and r_{cv}^2 associated with these CoMFA models for the training set compounds as protonated species were 0.96 and 0.68 for model 4 (Ts), 0.97 and 0.36 for model 5 (Tg), and 0.97 and 0.66 for model 6 (Cs). The r_{cv}^2 values for models 4 and 6 are well above the $r_{cv}^2 \geq 0.50$ criterion for predictive ability; yet, as found above, they are too similar to distinguish between these two models on the basis of statistical quality. The r_{cv}^2 value for model 5 falls below the $r_{cv}^2 \geq 0.50$ threshold and is considerably lower than the corresponding r_{cv}^2 values for models 4 and 6. Hence, comparison of the statistical parameters associated with these models (Table 5) suggests a stronger preference for the Ts and Cs conformers over the Tg conformer.

The CoMFA steric contour maps for models 1−6 (Figure 6) each depict that the N1 aromatic ring and C5 aromatic ring regions are important for steric interactions with the receptor. As indicated by the green contours near the N1 and C5 aromatic rings, increased

Table 5. Summary of Statistical Analysis and Field Contributions for CoMFA Models 1–6[a]

(a) assumed as unprotonated species

	CoMFA model 1 (Tg form)	CoMFA model 2 (Cg form)	CoMFA model 3 (Ts form)
Statistical Params			
r^2	0.97(6)	0.95(6)	0.96(6)
standard error of estimate (SEE)	0.158	0.219	0.179
F	123	63	95
P	<0.001	<0.001	<0.001
r_{cv}^2	0.68(6)	0.73(6)	0.69(6)
Field Contributions			
steric (%)	71	65	66
electrostatic (%)	29	35	34

(b) assumed as protonated species

	CoMFA model 4 (Ts form)	CoMFA model 5 (Tg form)	CoMFA model 6 (Cs form)
Statistical Params			
r^2	0.96(6)	0.97(6)	0.97(6)
SEE	0.193	0.170	0.177
F	82	107	97
P	<0.001	<0.001	<0.001
r_{cv}^2	0.68(6)	0.36(6)	0.66(6)
Field Contributions			
steric (%)	70	64	63
electrostatic (%)	30	36	37

[a] Values in parentheses are the number of principal components (PCs).

Table 6. Observed vs CoMFA-Predicted pK_i Values in Units of Nanomolar for Test Set Compounds

(a) assumed as unprotonated species

compd	pK_i (obsd)	CoMFA model 1 (Tg form) pK_i (pred)	CoMFA model 2 (Cg form) pK_i (pred)	CoMFA model 3 (Ts form) pK_i (pred)
31	−0.85	−1.40, −1.38[a]	−1.46, −1.36[a]	−1.75, −1.50[a]
32	−2.26	−2.12 ∼ −1.82[a]	−1.81 ∼ −1.79[a]	−2.10 ∼ −1.80[a]
33	−1.49	−1.03	−0.88	−1.27
34	−2.09	−0.70	−1.22	−1.22
35	−1.23	−0.81	−0.92	−1.04
36	−1.23	−0.56	−0.54	−0.73
37	−0.89	−0.60	−0.65	−0.64

(b) assumed as protonated species

compd	pK_i (obsd)	CoMFA model 1 (Ts form) pK_i (pred)	CoMFA model 2 (Tg form) pK_i (pred)	CoMFA model 3 (Cs form) pK_i (pred)
31	−0.85	−1.27, −1.22[a]	−1.37, −1.30[a]	−0.78[a]
32	−2.26	−1.97 ∼ −1.84[a]	−1.10 ∼ −0.70[a]	−2.51 ∼−1.76[a]
33	−1.49	−1.22	−1.47	−0.83
34	−2.09	−0.77	−0.20	−0.85
35	−1.23	−0.94	−0.68	−1.08
36	−1.23	−0.48	0.07	−0.62
37	−0.89	−0.53	−0.47	−0.89

[a] Values corresponding to different conformations.

binding affinities were predicted by introducing hydrophobic substituents on these rings. However, further extension of hydrophobic substituents beyond the immediate N1 ring structure is associated with decreased binding affinities, as denoted by the yellow contours in each of the three models. The N1 substituents associated with high binding affinity are 2,4-dichlorophenyl (as in **1**), *n*-pentyl (as in compound **15**), and *n*-hexyl (as

in compound **17**). These alkyl substituents, which can adopt a bent conformation and possibly occupy the receptor space similar to the 2,4-dichlorophenyl moiety, might be expected to interact with the same residues in the receptor binding pocket. It is interesting to note that a size limitation of the hydrophobic moiety has been similarly observed for the C3 side chain of cannabinoid compounds.[35] Therefore, it is plausible that the N1 aromatic ring moiety of **1** and the C3 side chain of cannabinoids interact with the same binding site, providing good hydrophobic interactions between the receptor and the ligand.

Analysis of the CoMFA electrostatic fields indicated that dipole−dipole or hydrogen-bonding interactions of the substituent on the C3 amide with the receptor are important for explaining the variation in binding affinity among these compounds for the receptor. Polar functional groups, such as the amide oxygen, the piperidine nitrogen, and other nitrogen or oxygen atoms (as in compounds **10**, **11**, and **19**−**21**) of the C3 substituent would appear as important for electrostatic interactions with the receptor. The contributions of electrostatic interactions with the receptor binding pocket are predicted to be larger in CoMFA models 2, 5, and 6 than in CoMFA models 1, 3, and 4, based on inspection of the CoMFA field contributions (Table 5) as well as the CoMFA contour maps. Interestingly, models 2 and 6 predicted that negative charge around the C3 substituent region of the molecule could attenuate binding interactions with the receptor. However, model 5, which was the least-preferred model among the protonated models, predicted that negative charge around the C3 substituent region of the molecule could augment binding interactions with the receptor.

The predictive ability of CoMFA models 1−6 was evaluated using a test set composed of compound **31**[15] and compounds **32**−**37** obtained from a recent SAR study.[16] The latter compounds were chosen by virtue of the consistency with the present study in terms of the binding data (Table 1). Compounds **35**−**37** (which vary with respect to the C3 amide substituents) were used to further evaluate CoMFA models 2, 5, and 6, since these CoMFA models depicted significant electrostatic contributions around the C3 amide substitution. CoMFA models 1−4 and 6 predicted binding affinities of the test set compounds within 1 log unit of the observed values except for compound **34**, while CoMFA model 5 was able to predict within 1 log unit only for **31** and compounds **33**, **35**, and **37**. These results for the test set compounds are consistent with the r_{cv}^2 values and other statistical parameters for the corresponding CoMFA models. Specifically, they suggest that the Tg, Cg, and Ts conformers considered in this study are equally valid in terms of possible biological relevance assuming that the compounds exist as unprotonated species. If, instead, the compounds are assumed to exist as protonated species, the Cs and Ts conformers are equally valid but the Tg conformer is less so.

Discussion

Superimposition Model. The approach we have taken to predict a mechanism for the arylpyrazole CB_1 cannabinoid receptor antagonists is based upon the assumption of an interaction with the receptor that is
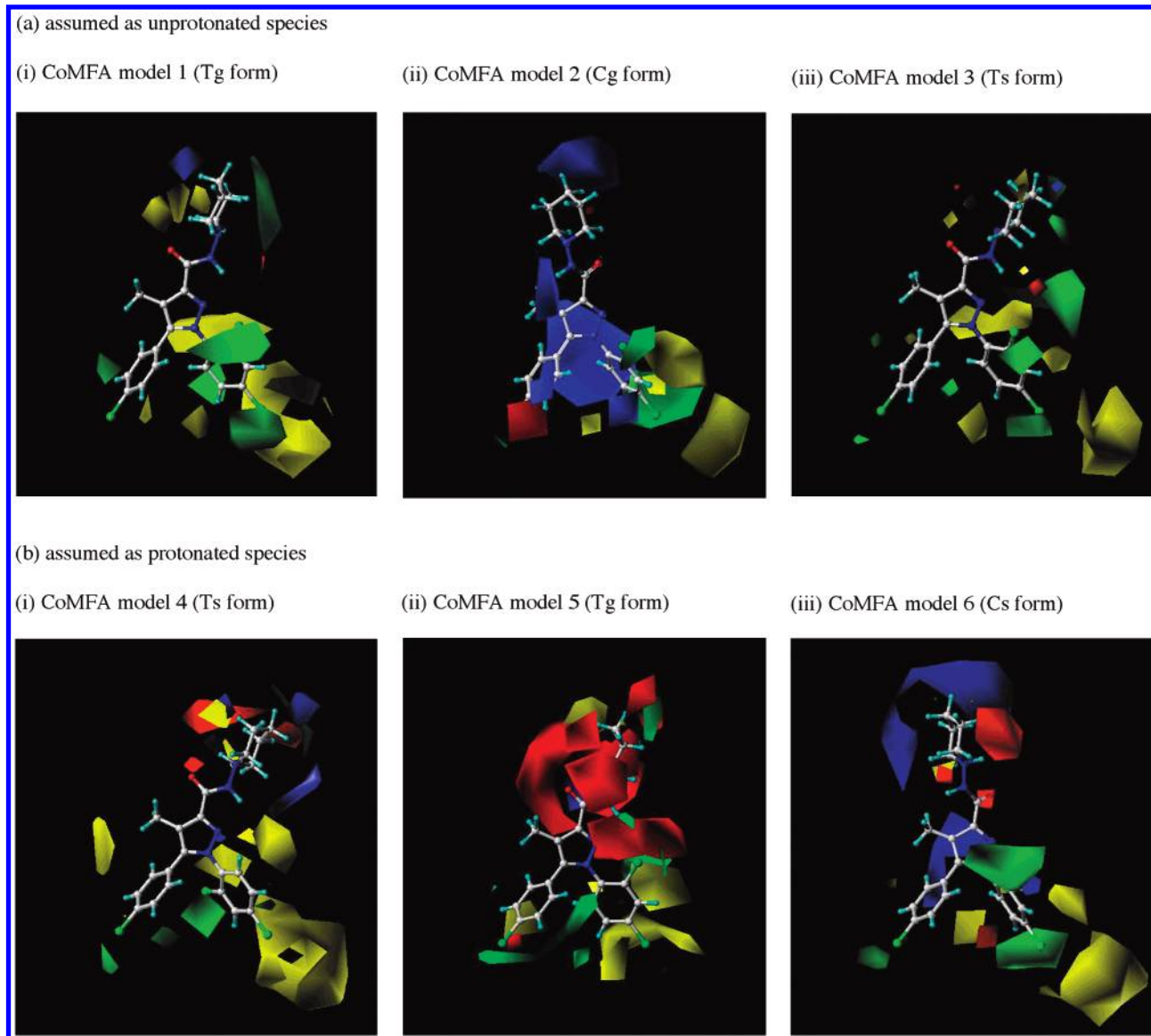
Figure 6. CoMFA steric and electrostatic contour plots for CoMFA models 1−6 from **1** and its 27 analogues with **1** used as the template molecule. CoMFA models 1−3 correspond, respectively, to the low-energy Tg, Cg, and Ts conformers of **1** assumed as an unprotonated species. CoMFA models 4−6 correspond, respectively, to the low-energy Ts, Tg, and Cs conformers of **1** assumed as a protonated species. The color contours describe regions determined from the training set compounds for which an increase in steric bulk of the molecule is predicted to enhance (green) and diminish (yellow) binding affinity for the receptor. Similarly, regions are depicted from the training set compounds for which an increase in negative charge of the molecule is predicted to enhance (red) or diminish (blue) binding affinity for the receptor.

competitive with agonist ligands. This assumption can be supported by corroborative lines of evidence. First, heterologous displacement curves can be generated for displacement of agonist radioligand ([³H]CP55940) by **1**.[7,8,15−17] Conversely, competitive displacement of [³H]-SR141716 by cannabinoid and AAI agonists has been demonstrated.[17,36,37] These displacements appear to exhibit properties typical of competitive interactions at the binding site. Furthermore, covalently bound ana-logues of **1** can preclude subsequent binding of [³H]-CP55940 after washout, suggesting co-occupation of a necessary common binding region.[18]

The superimposition models presented here are not the first to be proposed for **1** and cannabinoid agonists. Thomas et al.[17] developed a superimposition model from Δ⁹-THC and **1** based on their pharmacological analysis of a series of **1** analogues halogenated on the N1 aryl ring or C5 aryl ring. Their alignment rule included the

C5 aryl ring of **1** overlaid with the C3 pentyl side chain of Δ⁹-THC, the amide oxygen of **1** overlaid with the pyran oxygen in Δ⁹-THC, and the N2 of **1** overlaid with the phenolic hydroxyl oxygen of Δ⁹-THC. From their model, the N1 aryl moiety, which was unique for **1**, was proposed as the "antagonist-conferring" region of **1**. In contrast, our superimposition models involved aligning the N1 aryl moiety of **1** with the C3 side chain of cannabinoid compounds, leaving the C5 aryl ring as a unique moiety. Alternative strategies for antagonism might be proposed that allow for agonist and antagonist binding to distinctly different residues on the receptor, making a superimposition analysis irrelevant. To date, no definitive evidence for such a mechanism exists for the cannabinoid receptor. The present superimposition analysis, as well as that by Thomas et al.,[17] has demonstrated that low-energy conformations of **1** exist,

which can share some pharmacophoric elements with cannabinoid agonists.

Hypothetical Molecular Mechanism of 1. Hydrophobic interaction is an essential feature of ligand binding to the CB_1 cannabinoid receptor. As indicated from extensive SAR studies of cannabinoid compounds, the C3 side chain seems to be essential for receptor binding and agonist activity.[35,38] CoMFA analysis of a series of nonclassical cannabinoid structures indicated that 74% of the variation in affinity among the training set compounds was contributed by steric interactions.[31] Similarly, CoMFA analysis of AAI ligands indicates an 80% contribution from steric interactions.[32] Using **3** as a template, the C3 aroyl ring could subserve that interaction. All six CoMFA models concur that contributions from the steric fields (63–70%), which are substantially greater than those from the electrostatic fields, and that the region around the N1 aryl ring moiety are particularly important for steric interactions with the receptor (Figure 6).

From analysis of the present superimposition models, the N1 aryl ring moiety of **1** appears to engage in a hydrophobic interaction with the receptor. Accordingly, the 2,4-dichlorophenyl group of **1** would fit into the lipophilic pocket of the receptor. It is proposed that the cannabinoid C3 side chain, the AAI C3 aroyl ring moiety, and the **1** N1 aryl ring bind with the receptor through a hydrophobic interaction that is critical for initial docking of the ligand within the receptor binding pocket. Both superimposition models proposed here relegate the 4-chlorophenyl group as that moiety extending beyond the overlap volume in common with agonists. In the Thomas superimposition model,[17] the 4-chlorophenyl moiety overlaps with the cannabinoid C3 side chain proposed to be essential for hydrophobic docking, leaving the N1 aryl ring as the antagonist specific region. In either case, the excluded hydrophobic moiety may be hypothesized to interact with a specific region of the receptor and thereby to prohibit the conformational transitions in the receptor required for activation. On the basis of a SAR study of analogues of **1** with substituents on N1, C3, or C5, Wiley et al.[16] and Lan et al.[30] concluded in accordance with the above proposition that both of the substituents on N1 and C5 are crucial for the high affinity binding of **1** analogues.

Although there are regions noted in the superimposition models where electrostatic interactions with the receptor may be common to the cannabinoids, AAIs, and **1**, these do not necessarily coincide with the pharmacophoric points that have been previously proposed as important for agonist binding and activity.[19,31,32] For example, the C-ring hydroxyl of the cannabinoid agonists has been found to enhance binding; yet, this site does not appear as an area of overlap in superimposition model B. The substituents off the A-ring of the nonclassical AC-bicyclic and ACD-tricyclic cannabinoids are excluded from the overlap volume in both superimposition models. Among the AAIs, the indole nitrogen and both the morpholine nitrogen and the oxygen moieties have also been excluded from areas of overlap in both superimposition models. These regions of the agonist ligands may be involved in receptor interactions that induce or stabilize a conformation necessary for activation of G proteins. Such interactions are presumably

electrostatic in nature. Wiley et al.[30] have developed analogues of **1** that behave as agonists in biological assays. Modifications of these analogues were all localized to the C3 constituent of **1**. This would be consistent with this region of the molecule participating in the interactions with the receptor that induce or stabilize the active conformation.

On the basis of the superimposition models presented here, hydrogen bond acceptor atoms are found in close proximity to the receptor (i.e., the phenolic hydroxyl oxygen of cannabinoids, the C3 aroyl oxygen of AAIs, and the C3 amide oxygen of **1**). It has been proposed that the CB_1 receptor *Lys192* is involved in ligand binding to the receptor based upon a homologous amino acid in that position that is essential for binding to aminergic hormones.[39] Mutation studies on the CB_1 receptor suggest that a specific hydrogen-bonding interaction involving the *Lys192* side chain is critical for binding of the cannabinoids but not the AAIs.[39,40] Those researchers suggested that the phenolic hydroxyl of the cannabinoid structure serves as the hydrogen bond acceptor.[39] According to our superimposition model, protonation of **3** (on the morpholine N) and **1** (on the piperidine N) would be expected to eliminate or drastically weaken any putative hydrogen bonding between AAIs or analogues of **1** with the side chain of the *Lys192* residue, thereby reducing the relative importance of this putative hydrogen-bonding interaction to the ligand–receptor binding affinity for these classes of ligands.

Antagonist vs Inverse Agonist Activity. Considerable evidence is accruing to suggest that **1** may exhibit inverse agonist activity in model systems[13–15] and perhaps in neurons within the brain. This would imply that **1** can induce or stabilize a conformation of the receptor necessary for the inverse agonist behavior. We have proposed several alternative low-energy conformations that are possible for **1** to attain in situ. On the basis of the present modeling study, three conformers (Tg, Cg, and Ts) for the charge-neutral antagonist molecule and two conformers (Ts and Cs) for the piperidine N protonated molecule were identified that represent low-energy conformations and that are associated with statistically robust and predictive CoMFA models. Once the molecule has docked within the receptor pocket driven by steric interactions, it is plausible that subsequent interactions with specific negatively charged amino acid residues (as suggested by the blue contour in Figure 6b i,iii) may promote deprotonation, which in turn would destabilize the protonated Ts or Cs conformation in favor of the unprotonated Tg or Cg conformation. The Tg conformer of the protonated species yielded less predictive CoMFA models and, therefore, might be judged less viable as a binding conformation. Nevertheless, one could conceive of a dynamic conformational interaction with the receptor in which **1** initially binds in the unprotonated Tg conformation. Then, ion-bridging with a glutamic acid residue (e.g., Glu 258) could facilitate a protonated state with concomitant conversion to the highly preferred Ts form. It is interesting to notice that the CoMFA electrostatic contour maps for models 2 and 6 show similar blue polyhedra around the C3 amide of the antagonist indicating that the unprotonated Cg form and protonated Cs form interconvert dynamically within an

identical receptor environment. Alternatively, conversion between the unprotonated Tg and Cg or the protonated Ts and Cs in vivo, if these are two major forms, would be easily achieved, as suggested by the surmountable rotational barrier for **1** with respect to torsion angle $\omega2$ (N2=C3−C=O) (approximately 5 kcal/mol by the AM1 method). As reflected in the corresponding CoMFA models (Figure 6), these two forms depict very different electrostatic fields, especially around the C3 amide substituent region. Thus, **1** may confer dynamic interactions with amino acid residues in the receptor's binding pocket that could be responsible for mediating inverse agonist activity.

In summary, we believe that the N1 or C5 aryl ring moiety is important for hydrophobic docking into receptor pocket, a property of binding in common with agonists. Subsequently, the steric forces of the second ring may prohibit any receptor conformational change necessary for agonist activity. We hypothesize, more importantly, that the C3 amide substituent is important not only to prohibit agonist activity but also to induce or stabilize a receptor conformation necessary for inverse agonist activity.

References

(1) Abood, M. E.; Martin, B. R. Neurobiology of marijuana abuse. *Trends Pharmacol. Sci.* **1992**, *13*, 201−206.

(2) Hollister, L. E. Health aspects of cannabis. *Pharmacol. Rev.* **1986**, *38*, 1−20.

(3) Howlett, A. C. Pharmacology of cannabinoid receptors. *Annu. Rev. Pharmacol. Toxicol.* **1995**, *35*, 607−634.

(4) Felder, C. C.; Glass, M. Cannabinoid receptors and their endogenous agonists. *Annu. Rev. Pharmacol. Toxicol.* **1998**, *38*, 179−200.

(5) Howlett, A. C. The CB$_1$ cannabinoid receptor in the brain. *Neurobiol. Dis.* **1998**, *6* (Pt. B), 405−416.

(6) Barth, F.; Rinaldi-Carmona, M. The development of cannabinoid antagonists. *Curr. Med. Chem.* **1999**, *6*, 745−755.

(7) Rinaldi-Carmona, M.; Barth, F.; Héaulme, M.; Shire, D.; Calandra, B.; Congy, C.; Martinez, S.; Maruani, J.; Neliat, G.; Caput, D.; Ferrara, P.; Soubrie, P.; Breliere, J. C.; Le Fur, G. SR141716A, A potent and selective antagonist of the brain cannabinoid receptor. *FEBS Lett.* **1994**, *350*, 240−244.

(8) Rinaldi-Carmona, M.; Barth, F.; Héaulme, M.; Alonso, R.; Shire, D.; Congy, C.; Soubrié, P.; Breliere, J.-C.; Le Fur, G. Biochemical and pharmacological characterization of SR141716A, the first potent and selective brain cannabinoid receptor antagonist. *Life Sci.* **1995**, *56*, 1941−1947.

(9) Lichtman, A. H.; Martin, B. R. The selective cannabinoid antagonist SR141716A blocks cannabinoid-induced antinociception in rats. *Pharmacol. Behav.* **1997**, *57*, 7−12.

(10) Wiley, J. L.; Barrett, R. L.; Lowe, J. A.; Balster, R. L.; Martin, B. R. Discriminative stimulus effects of CP55,940 and structurally dissimilar cannabinoids in rats. *Neuropharmacology* **1995**, *34*, 669−676. (b) Wiley, J. L.; Lowe, J. A.; Balster, R. L.; Martin, B. R. Antagonism of the discriminative stimulus effects of Δ-9-tetrahydrocannabinol in rats and rhesus monkeys. *J. Pharmacol. Exp. Ther.* **1995**, *275*, 1−6.

(11) Tsou, K.; Patrick, S. L.; Walker, J. M. Physical withdrawal in rats tolerant to Δ-9-tetrahydrocannabinol precipitated by a cannabinoid receptor antagonists. *Eur. J. Pharmacol.* **1995**, *280*, R13−R15.

(12) Aceto, M. D.; Scates, S. M.; Lowe, J. A.; Martin, B. R. Cannabinoid precipitated withdrawal by the selective cannabinoid receptor antagonist, SR141716A. *Eur. J. Pharmacol.* **1995**, *282*, R1−R2.

(13) Bouaboula, M.; Perrachon, S.; Milligan, L.; Canat, X.; Rinaldi-Carmona, M.; Portier, M.; Barth, F.; Calandras, B.; Pecceu, F.; Lupker, J.; Maffrand, J.-P.; Le Fur, G.; Casellas, P. A selective inverse agonist for central cannabinoid receptor inhibits mitogen-activated protein kinase activation stimulated by insulin or insulin-like growth factor. 1. Evidence for a new model of receptor/ligand interactions. *J. Biol. Chem.* **1997**, *272*, 22330−22339.

(14) Landsman, R. S.; Burkey, T. H.; Consroe, P.; Roeske, W. R.; Yamamura, H. I. SR141716A is an inverse agonist at the human cannabinoid CB$_1$ receptor. *Eur. J. Pharmacol.* **1997**, *334*, R1−R2.

(15) Meschler, J. P.; Kraichely, D. M.; Wilken, G. H.; Howlett, A. C. Inverse agonist properties of *N*-(piperidin-1-yl)-5-(4-chlorophenyl)-1-(2,4-dichlorophenyl)-4-methyl-1H-pyrazole-3-carboxamide HCl (SR141716A) and 1-(2-chlorophenyl)-4-cyano-5-(4-methoxyphenyl)-1H-pyrazole-3-carboxylic acid phenylamide (CP-272871) for the CB$_1$ cannabinoid receptor. *Biochem. Pharmacol.* **2000**, *60*, 1315−1323.

(16) Lan, R.; Liu, Q.; Fan, P.; Lin, S.; Fernando, S. R.; McCallion, D.; Pertwee, R.; Makriyannis, A. Structure−activity relationships of pyrazole derivatives as cannabinoid receptor antagonists. *J. Med. Chem.,* **1999**, *42*, 769−776.

(17) Thomas, B. F.; Gilliam, A. F.; Burch, D. F.; Roche, M. J.; Seltzman, H. H. Comparative receptor binding analyses of cannabinoid agonists and antagonists. *J. Pharmacol. Exp. Ther.* **1998**, *285*, 285−292.

(18) Howlett, A. C.; Wilken, G. H.; Pigg, J. J.; Houston, D. B.; Lan, R.; Liu, Q.; Makriyannis, A. Azido- and isothiocyanato-substituted arylpyrazoles bind covalently to the CB$_1$ cannabinoid receptor and impair signal transduction. *J. Neurochem.* **2000**, *74*, 2174−2181.

(19) Shim, J.-Y.; Collantes, E. R.; Welsh, W. J.; Howlett, A. C. United pharmacophoric model for cannabinoids and aminoalkylindoles derived from molecular superimposition of CB$_1$ cannabinoid receptor agonists CP55244 and WIN55212-2. In *Rational Drug Design Symposium Series*; Parrill, A. L., Reddy, M. R., Eds.; American Chemical Society: Washington, DC, 1999; pp 165−184.

(20) Cramer, R. D., III; Patterson, D. E.; Bunce, J. D. Comparative molecular field analysis (CoMFA). 1. Effect of shape on binding of steroids to carrier proteins. *J. Am. Chem. Soc.* **1988**, *110*, 5959−5967.

(21) Wavefunction, Inc.; Irvine, CA 92612.

(22) Dewar, M. J. S.; Zoebisch, E. G.; Healy, E. F.; Stewart, J. J. P. AM1: A new general purpose quantum mechanical molecular model. *J. Am. Chem. Soc.* **1985**, *107*, 3902−3909.

(23) Goto, H.; Osawa, E. An efficient algorithm for searching low-energy conformers of cyclic and acyclic molecules. *J. Chem. Soc., Perkin Trans. 2* **1993**, 187−198.

(24) Halgren, T. A. Merck molecular force field. I. Basis, form, scope, parametrization, and performance of MMFF94. *J. Comput. Chem.* **1996**, *17*, 490−519.

(25) Martin, Y.; Bures, M. G.; Danaher, E. A.; DeLazzer, J.; Lico, I.; Pavlik, P. A. A fast approach to pharmacophore mapping and its application to dopaminergic and benzodiazepine agonists. *J. Comput.-Aided Mol. Des.* **1993**, *7*, 83−102.

(26) Tripos, Inc.; St. Louis, MO 63144.

(27) Gasteiger, J.; Marsili, M. Iterative partial equalization of orbital electronegativity: a rapid access to atomic charges. *Tetrahedron* **1980**, *36*, 3219−3228.

(28) Wold, S.; Albano, C.; Dunn, W. J., III; Edlund, U.; Esbensen, K.; Geladi, P.; Hellberg, S.; Johansson, E.; Lindberg, W.; Sjostrom, M. Multivariate data analysis in chemistry. In *Chemometrics: Mathematics and Statistics in Chemistry*; Kowalski, B., Ed.; Reidel: Dordrecht, The Netherlands, 1984.

(29) Cramer, R. D., III; Bunce, J. D.; Patterson, D. E. Crossvalidation, bootstrapping, and partial least squares compared with multiple regression in conventional QSAR studies. *Quant. Struct.-Act. Relat.* **1988**, *7*, 18−25.

(30) Wiley, J. L.; Jefferson, R. G.; Grier, M. C.; Mahadevan, A.; Razdan, R. K.; Martin, B. R. Novel pyrazole cannabinoids: insights into CB$_1$ receptor recognition and activation. *J. Pharmacol. Exp. Ther.* **2001**, *296*, 1013−1022.

(31) Tong, W.; Collantes, E. R.; Welsh, W. J.; Berglund, B. A.; Howlett, A. C. Derivation of a pharmacophore model for anandamide using constrained conformational searching and comparative molecular field analysis. *J. Med. Chem.* **1998**, *41*, 4207−4215.

(32) Shim, J.-Y.; Collantes, E. R.; Welsh, W. J.; Subramaniam, B.; Howlett, A. C.; Eissenstat, M. A.; Ward, S. J. Three-dimensional quantitative structure−activity relationship study of the cannabimimetic (aminoalkyl)indoles using comparative molecular field analysis (CoMFA). *J. Med. Chem.* **1998**, *41*, 4521−4532.

(33) Xie, X. Q.; Yang, D. P.; Melvin, L. S.; Makriyannis, A. Conformational analysis of the prototype nonclassical cannabinoid CP-47,497 using 2D NMR and computer molecular modeling. *J. Med. Chem.* **1994**, *37*, 1418−1426.

(34) Keimowitz, A. R.; Martin, B. R.; Razdan, R. K.; Crocker, P. J.; Mascarella, S. W.; Thomas, B. F. QSAR analysis of Δ^8-THC analogues: Relationship of side-chain conformation to cannabinoid receptor affinity and pharmacological potency. *J. Med. Chem.* **2000**, *43*, 59−70.

(35) Melvin, L. S.; Milne, G. M.; Johnson, M. R.; Subramaniam, B.; Wilken, G. H.; Howlett, A. C. Structure−activity relationships for cannabinoid receptor-binding and analgesic activity: Studies of bicyclic cannabinoid analogues. *Mol. Pharmacol.* **1993**, *44*, 1008−1015.

(36) Houston, D. B.; Howlett, A. C. Differential receptor-G-protein coupling evoked by dissimilar cannabinoid receptor agonists. *Cell. Signalling* **1998**, *10*, 667−674.

(37) Rinaldi-Carmona, M.; Calandra, B.; Shire, D.; Bouaboula, M.; Oustric, D.; Barth, F.; Casellas, P.; Ferrara, P.; Le Fur, G. Characterization of two cloned human CB_1 cannabinoid receptor isoforms. *J. Pharmacol. Exp. Ther.* **1996**, *278*, 871−878.

(38) Razdan, R. K. Structure−activity relationships in cannabinoids. *Pharmacol. Rev.* **1986**, *38*, 75−149.

(39) Song, Z.-H.; Bonner, T. I. A lysine residue of the cannabinoid receptor is critical for receptor recognition by several agonists but not WIN55212-2. *Mol. Pharmacol.* **1996**, *49*, 891−895.

(40) Chin, C.; Abadji, V.; Lucas-Lenard, J.; Kendall, D. Ligand binding and modulation of cyclic AMP levels depends on the chemical nature of the residue 192 of the human cannabinoid receptor 1. *J. Neurochem.* **1998**, *70*, 366−373.